

## Effects of A-Site and B-Site Vacancies on Structural and Dielectric Properties of PLZT Ceramics

Cheol-Su Jeong, Hyu-Bum Park, Young-Sik Hong and Si-Joong Kim

Department of Chemistry, Korea University, Seoul 136-701, Korea

(Received June 1, 1996)

PLZT ceramics having two nominal compositions,  $Pb_{1-3x/2}La_xV_{x/2}(Zr_{0.5}Ti_{0.5})O_3$  and  $Pb_{1-x}La_x(Zr_{0.2}Ti_{0.8})_{1-x/4}V_{x/4}O_3$  (V: vacancy) with  $x=0.00\sim 0.30$ , were prepared. The physical, structural, and dielectric properties were investigated by X-ray diffraction, scanning electron microscopy, Raman spectroscopy, and measurements of bulk density and dielectric constant. The two series with A-site and B-site vacancies showed different physical, structural, dielectric properties, and, specially, Curie temperature. In comparison to PLZT with B-site vacancies, PLZT with A-site vacancies showed high Curie temperatures and low maxima of dielectric constant. Consequently, it is evident that the properties of PLZT ceramics depend on the vacancy formula adopted as a batch composition in preparation.

**Key words** : PLZT, A- and B-site vacancies, Structural and dielectric properties

### I. Introduction

Lanthanum-modified lead zirconate titanate (PLZT) ceramics are perovskite-type ferroelectrics with good electrooptic characteristics and have been extensively studied for many applications such as shutter, modulator, and image storage devices.<sup>1,2)</sup> It is also well known that lead zirconate titanate (PZT) forms a homogeneous perovskite solid solution for the whole range of Zr/Ti ratio.<sup>3,4)</sup> However, most investigations for the lanthanum-modified PZT system have been concentrated on Zr-rich region, especially, near the morphotropic phase boundary between rhombohedral and tetragonal ferroelectric phases.<sup>5-7)</sup>

In PLZT system, since the  $La^{3+}$  ions enter  $Pb^{2+}$  ion sites due to their ionic sizes,<sup>8)</sup> the excess positive charges caused by the introduction of the trivalent ions must be compensated. Hårdtl and Hennings<sup>9)</sup> suggested that the excess charge could be compensated by the formations of both A-site and B-site vacancies in the perovskite lattice. Two possible vacancy formulas can be expressed in the following forms:

$Pb_{1-3x/2}La_xV_{x/2}(Zr/Ti)O_3$  ----- A-site vacancy formula

$Pb_{1-x}La_x(Zr/Ti)_{1-x/4}V_{x/4}O_3$  ----- B-site vacancy formula

where V represents a vacancy. The distribution of A-site and B-site vacancies in the PLZT system has not yet been completely resolved. Nevertheless, it is generally accepted that A-site vacancies are predominant in Zr-rich region and the amount of B-site vacancy increases with increasing Ti content.<sup>1,9)</sup>

Although the defect structure of PLZT is complex and, moreover, has not yet been completely understood, the B-site vacancy formula has been usually adopted as a

batch composition by many investigators to compensate PbO loss during sintering process and to obtain transparent ceramics.<sup>5-7,10,11,13)</sup> In fact, the B-site vacancy formula has more PbO content than the A-site vacancy formula. In Pb-containing ferroelectrics, the PbO content is known to be an important factor on their physical and dielectric properties.<sup>11-13)</sup> In addition, the above two formulas have different types of defect structures and, in each formula, the increase of  $La^{3+}$  substitution increases the amount of A- or B-site vacancies, respectively. Therefore, the two ceramic series are expected to show different physical, structural and dielectric properties.

In the present work, we prepared PLZT ceramics with Zr/Ti=20/80 and  $x=0.00\sim 0.30$  according to two vacancy formulas and investigated the differences in properties between A- and B-site vacancy formula. It was found that the physical, structural, and dielectric properties, such as tetragonality, unit cell volume, bulk density, Raman scattering, dielectric constant, and Curie temperature, were dependent on the vacancy formula.

### II. Experimental Procedure

The PLZT samples were prepared according to two nominal compositions,  $Pb_{1-3x/2}La_xV_{x/2}(Zr_{0.5}Ti_{0.5})O_3$  (PLZT-A) and  $Pb_{1-x}La_x(Zr_{0.2}Ti_{0.8})_{1-x/4}V_{x/4}O_3$  (PLZT-B) with  $x=0.00\sim 0.30$ , corresponding to A-site and B-site vacancy formula, respectively. No excess PbO was added in all the samples. Reagent-grade oxides, PbO,  $La_2O_3$ ,  $ZrO_2$ , and  $TiO_2$  were ball-milled with ethyl alcohol for 24 h, dried, and calcined at 900°C for 2 h. The calcined powders were ground, and polyvinyl alcohol (3 wt.%) was added to facilitate pressing. The materials were pressed into disks and were placed within a series of  $Al_2O_3$  crucibles, as

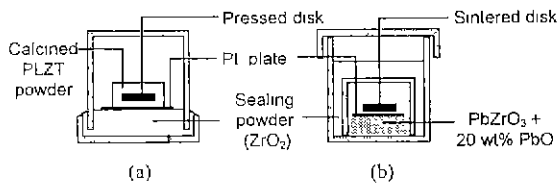


**Fig. 1.** Crucible arrangements for (a) sintering of pressed PLZT disks and (b) weight change test of the sintered disks under high partial pressure of PbO.

shown in figure 1(a), and sintered at 1300°C for 2 h. To minimize deviation from the originally formulated composition due to PbO evaporation, the disks were thickly covered with the calcined powders having same compositions. The calcined powder was removed after sintering and used to measure physical and structural properties. To check PbO contents of the sintered samples, the weight change test was subsequently carried out by annealing the sintered disks under the PbO-rich atmosphere (Fig. 1(b)).

X-ray diffraction (XRD) patterns for the sintered bodies were obtained using Cu-K $\alpha$  radiation with Ni filter. Bulk densities of the sintered disks were also measured by the Archimedes method. The surfaces of the sintered disks were observed by scanning electron microscopy (SEM; Jeol, JSM 840 A) and grain sizes were calculated by the linear-intercept method.<sup>14</sup> Raman spectra were recorded by Inova series 90 using argon laser as a source. For measurements of dielectric properties, the disks were electroded with silver paste and fired at 600°C. The dielectric constant was measured by LCR meter (Kokuyo, KC-536) at 10 kHz with increasing temperature.

### III. Results and Discussion

#### 1. Structural and physical properties

Phase analysis for the sintered disks was carried out by XRD. All the samples according to both PLZT-A and PLZT-B formulas showed XRD patterns of single perovskite phase. Table 1 lists calculated lattice parameters, tetragonalities ( $c/a$ ), and unit cell volumes. Figure 2 shows the variations of lattice parameters as a function of La content at room temperature. For both PLZT-A and PLZT-B, the crystal tetragonalities decrease smoothly with increasing La content ( $x$ ), and the samples with the composition of  $x=0.00-0.20$  are tetragonal, whereas those of  $x=0.25$  and  $0.30$  are cubic. These results agree with the phase diagrams of PLZT system reported by Hartling<sup>10</sup> and Schulze.<sup>4</sup> The unit cell volume was found to decrease with increasing La content for both PLZT-A and PLZT-B (Fig. 3). This indicates that for both formulas the La<sup>3+</sup> ions (1.032Å) enter Pb<sup>2+</sup> sites (1.19Å) rather than B sites (Ti: 0.605Å, Zr: 0.72Å).<sup>15</sup> It is well known in PLZT system that the unit cell volume and the tetragonality decrease as La content increases.<sup>1,10</sup>

To check PbO content of two series, we measured

**Table 1.** Lattice Parameters (Å), Tetragonalities ( $c/a$ ), and Unit Cell Volumes (Å<sup>3</sup>) for A-Site and B-Site Vacancy Formulas of PLZT

La (mol%)	PLZT-A				PLZT-B			
	a	c	Tetragonality ( $c/a$ )	Cell volume	a	c	Tetragonality ( $c/a$ )	Cell volume
0.0	3.950	4.145	1.049	64.67	3.950	4.145	1.049	64.67
5.0	3.954	4.103	1.038	64.15	3.960	4.089	1.033	64.12
13.0	3.961	4.049	1.022	63.53	3.967	4.047	1.020	63.69
20.0	3.964	4.012	1.012	63.04	3.973	4.002	1.007	63.17
25.0	3.965			62.33	3.975			62.81
30.0	3.958			62.01	3.971			62.62

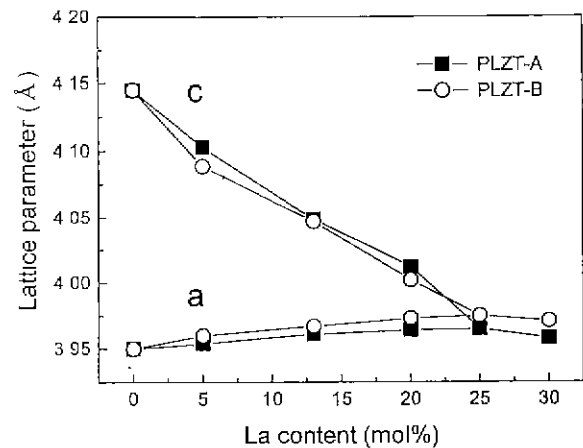


**Fig. 2.** Lattice parameters of PLZT-A and PLZT-B as a function of La content.

weight changes for several compositions before and after annealing the sintered disks under PbO rich atmosphere (figure 1(b)). The results are shown in figure 4. It was found that PLZT-A always gained weight, whereas PLZT-B gained weight below 10 mol% ( $x=0.10$ ) and then lost weight above 13 mol% ( $x=0.13$ ) even under PbO rich atmosphere. Thus, as expected from two vacancy formulas, the PLZT-A has relatively low PbO content than PLZT-B and the difference in PbO content increases as La content increases. By the weight change tests, although we could not know absolute defect structures of the samples, it was at least evident that PLZT-B had more PbO than PLZT-A in sintered bodies and, furthermore, the compositions of two series prepared in this study were considerably reliable.

By comparison of XRD results for two series, it was additionally observed that there were slight differences in unit cell volume and tetragonality between two series. PLZT-A has smaller unit cell volumes and larger tetragonalities than PLZT-B (Table 1) and the difference in unit cell volume generally increases with La content (figure 3). It was reported that for PLZT of 9/65/35 (La/Zr/Ti) composition the lattice parameter and Curie temperature ( $T_c$ ) increased with the increase of PbO content.<sup>11</sup>

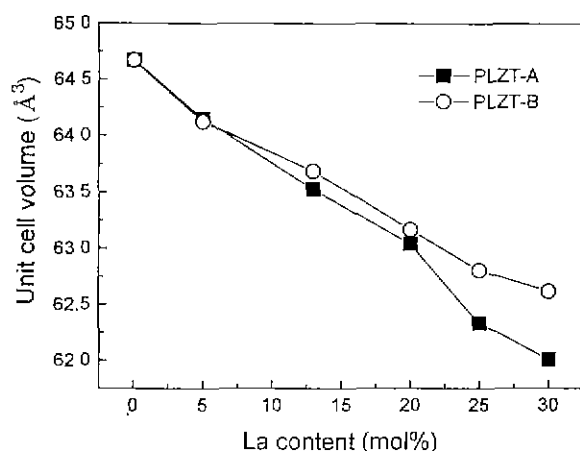


Fig. 3. Unit cell volumes of PLZT-A and PLZT-B as a function of La content.

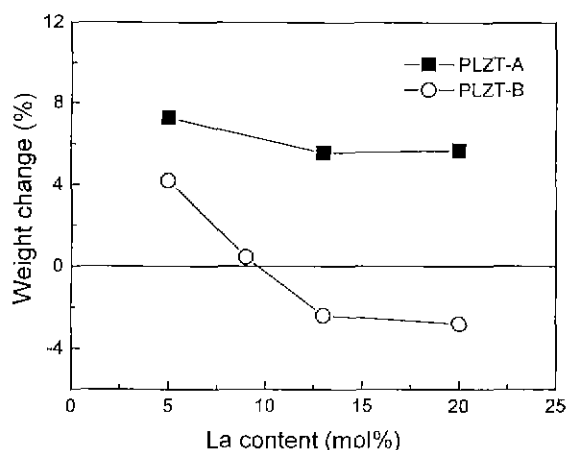


Fig. 4. Weight changes of PLZT-A and PLZT-B before and after annealing sintered disks.

Shirasaki *et al.*<sup>16</sup> also reported that in  $\text{PbTiO}_3$ , the unit cell volume, tetragonality, and  $T_c$  were inversely proportional to  $\text{PbO}$  deficiency in lattice. The difference in unit cell volume therefore can be possibly explained by that of  $\text{PbO}$  content, whereas the difference in tetragonality showing contradictory tendency is difficult to explain only by  $\text{PbO}$  content. In their systems,  $\text{PbO}$  concentrations in samples were simply changed, but, in our system, each concentration of A- or B-site vacancies in addition to  $\text{PbO}$  concentration, simultaneously increases in PLZT-A and PLZT-B, respectively, as La content increases. Thus, it is reasonable that the type and concentration of vacancy must be considered to explain the differences in unit cell volume and tetragonality. Unfortunately, the roles of each type vacancy on the structure in PLZT system have been hardly discussed in the literature and so it is still difficult to elucidate this phenomena. Nevertheless, it could be demonstrated from XRD results that the structural differences between PLZT-A and PLZT-B apparently appeared and seem to result from two different vacancy formulas.

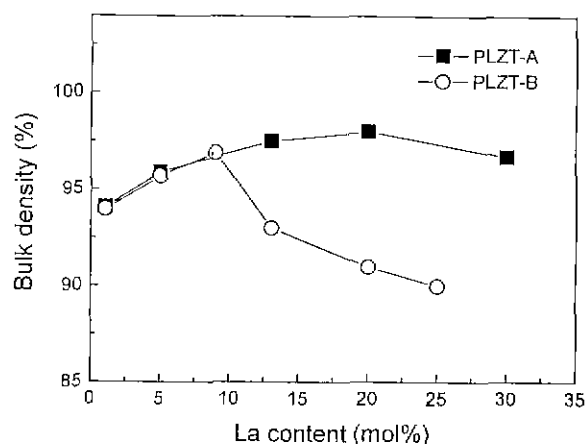


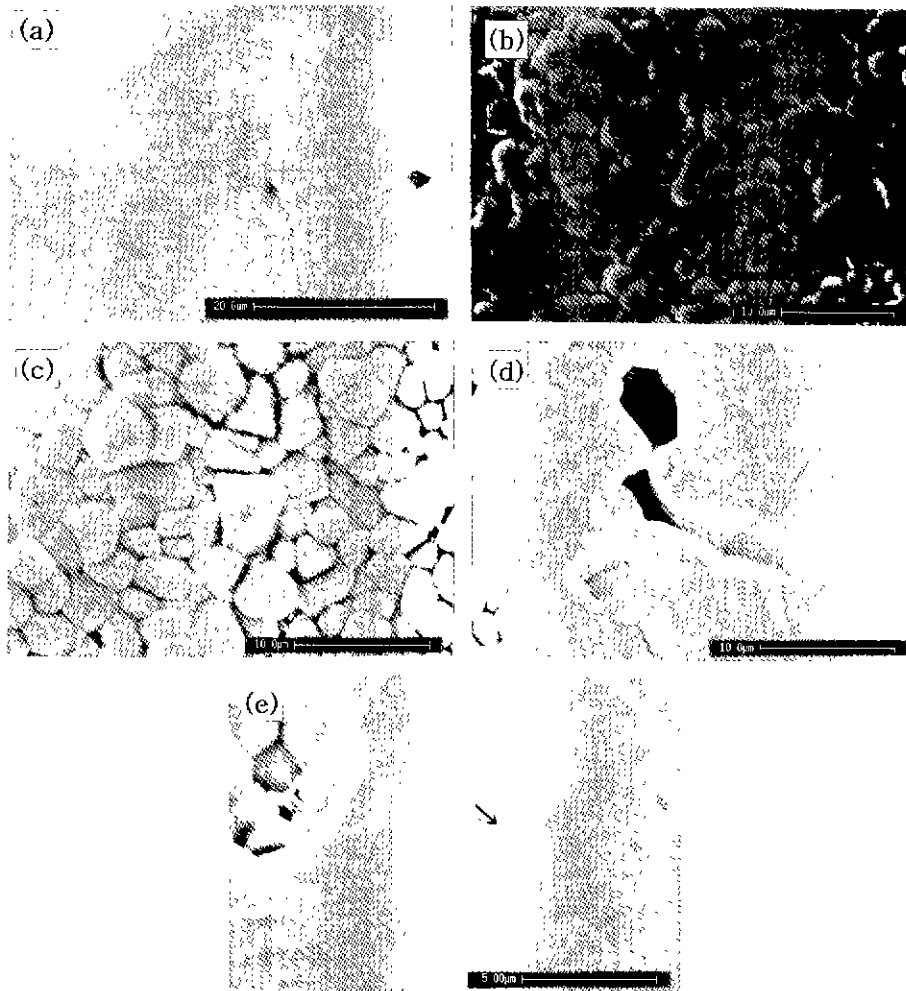
Fig. 5. Bulk density of sintered disks as a function of La content for PLZT-A and PLZT-B.

Figure 5 shows that the bulk densities of PLZT-A are higher than those of PLZT-B for higher La content region. The lower densities of PLZT-B may be ascribed to higher  $\text{PbO}$  contents. Song *et al.*<sup>17</sup> reported that, although excess  $\text{PbO}$  was necessary to aid sintering, too much excess  $\text{PbO}$  produced large pores in sintered body, and so reduced bulk density. Therefore, PLZT-B containing more excess  $\text{PbO}$  has lower bulk densities than PLZT-A in the higher La content region.

In addition, figure 6 (e) shows needle-like crystals, designated by arrow, on the surface of sintered body at 30 mol% La of PLZT-A, although any impurity phase was not detected by XRD. But, no second phase was observed in PLZT-B. From the appearance of second phase in PLZT-A, it is suspected that A-site vacancy is less soluble in PLZT lattice than B-site vacancy and also the PLZT-A formula is less stable for substitution of La into PZT lattice.

The grain size in each series significantly decreased at low La contents, and it reached a minimum at 9 mol% of La, and then slowly increased (figure 7). The decrease of grain size has been frequently observed when foreign ions, for example,  $\text{Ag}^+$ ,  $\text{Al}^{3+}$ ,  $\text{Nb}^{5+}$ , and  $\text{Bi}^{3+}$ , were incorporated into PZT lattice.<sup>17-19</sup> Atkin and Fulrath<sup>18</sup> explained that the grain size was reduced by the doping ions concentrated near grain boundary, which inhibited grain boundary movement. The slow increase of grain size in the range above 9 mol% can be understood by considering  $\text{PbO}$  content. By weight change tests, it was confirmed that PLZT-B had higher  $\text{PbO}$  content than PLZT-A and the difference in  $\text{PbO}$  content increased with increasing La content. As a result, the grain growth in PLZT-B containing more  $\text{PbO}$  was more strongly promoted by the formation of liquid phase due to  $\text{PbO}$  with low melting point ( $886^\circ\text{C}$ ) and thus the grain size was enlarged.

## 2. Raman spectroscopy



**Fig. 6.** SEM photographs for (a) 0 mol% La, (b) 5 mol% La, (c) 16 mol% La, and (d) 30 mol% La of PLZT-B, and (e) 30 mol% La of PLZT-A.

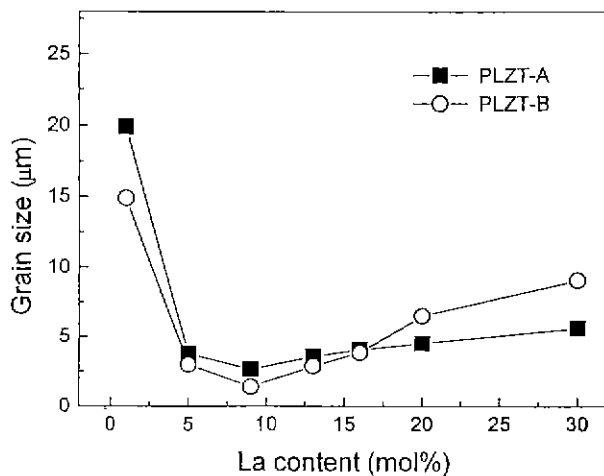


**Fig. 7.** Grain size of sintered disks as a function of La content for PLZT-A and PLZT-B.

Raman scattering is more sensitive than XRD to local site symmetry in perovskite-type crystal lattice.<sup>20,21</sup> To

find the difference of local structure between two series, Raman spectra were measured and are shown in figure 8 and figure 9. Burns et al.<sup>22,24</sup> intensively studied Raman scattering for  $\text{PbTiO}_3$ , PZT and PLZT. Our Raman data are in good agreements with the results published by them.<sup>23,24</sup> Thus, the phonon modes were identified by comparison with their data and the assigned modes are shown in figures.

In both series, the samples with low La contents showed typical spectra of tetragonal perovskite and each two modes ( $A_1(3\text{TO})$  and  $E(3\text{TO})$  modes) were gradually merged into single peaks as La contents increase. Taguchi et al.<sup>25</sup> reported that the Raman spectra for thin film of  $\text{PbTiO}_3$  changed in the same manner with increasing temperature, as a result of continuous transition from tetragonal to cubic phase. Therefore, it is clear that the merging phenomena with increasing La content resulted from the phase transition from tetragonal to cubic, as observed in XRD. It was also found by precise comparison that, with the increase of La content,  $A_1(3\text{TO})$  mode in PLZT-B is more rapidly combined with  $E(3\text{TO})$  mode

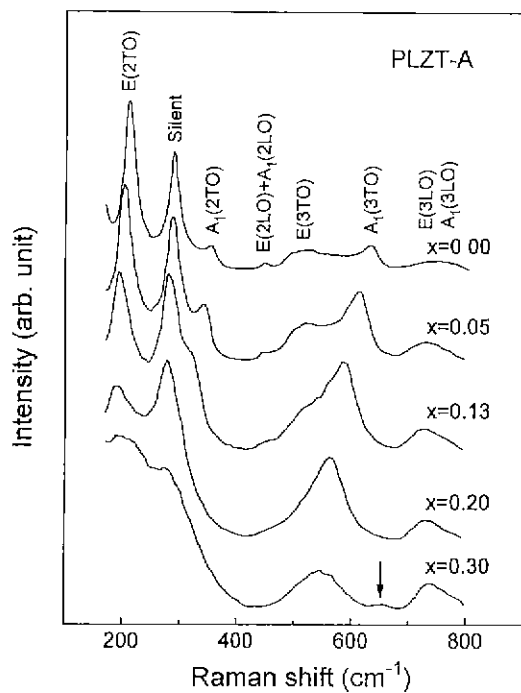


Fig. 8. Raman spectra of PLZT-A with various La contents.

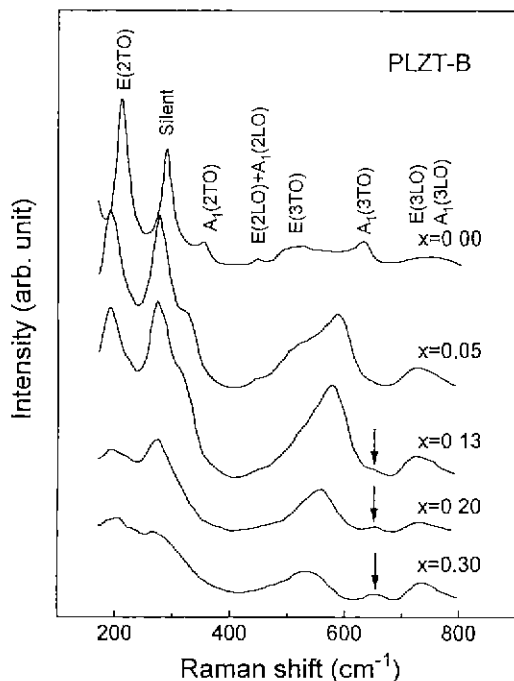


Fig. 9. Raman spectra of PLZT-B with various La contents.

than that in PLZT-A. This result can be similarly explained by considering the magnitude of tetragonality. That is, PLZT-B with low tetragonality shows more rapid combination than PLZT-A.

According to group theoretical treatments of Burns<sup>23)</sup> and Taguchi,<sup>25)</sup> tetragonal phase has twelve Raman-active modes, but cubic phase has no Raman-active mode.

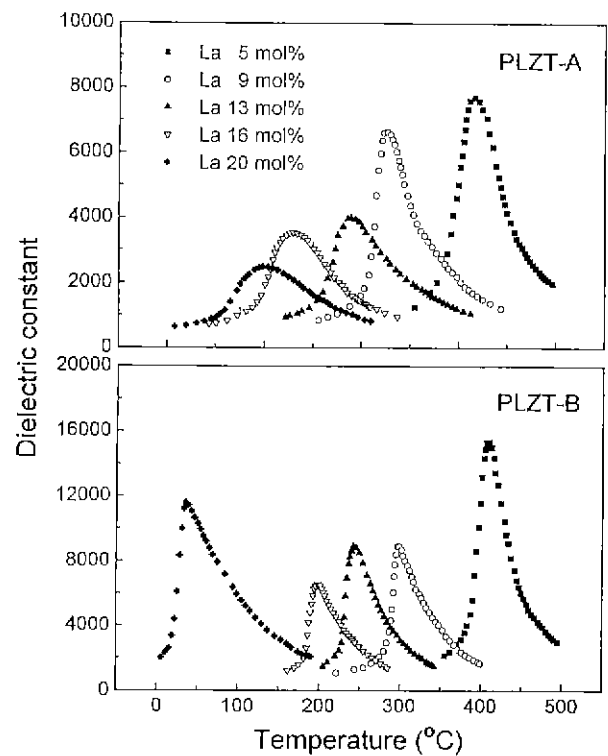


Fig. 10. Temperature dependences of dielectric constant of PLZT-A and PLZT-B with various La contents.

In this regard, the peaks of samples with 30 mol% La in cubic symmetry are expected to disappear but still remained. Consequently, it can be indicated that, in PLZT lattice, there is a distortion of local site symmetry possibly due to the formation of vacancy, which cannot be detected by XRD.

Furthermore, although there was little difference of Raman spectra between PLZT-A and PLZT-B, a small peak designated by arrow in figures appeared at about 650  $\text{cm}^{-1}$  and the peak intensity for PLZT-B more rapidly increased than PLZT-A. Brya<sup>25)</sup> demonstrated that the small peak was believed to be an impurity mode associated with incorporation of  $\text{La}^{3+}$  into perovskite lattice. Accordingly, it was revealed by Raman scattering that the introduction of La ions into PZT lattice had different effects on the local site symmetry in each formula, which might be attributed to the formation of two different types of vacancies in PLZT lattice.

### 3. Dielectric properties

Dielectric constant (K) was measured at 10 kHz with increasing temperature up to 500°C. Temperature dependences of dielectric constant for two series are shown in figure 10. It can be seen that PLZT-B gives greater peak heights for all samples having the same mol% of La than PLZT-A. In PLZT and PZT systems the maximum dielectric constant ( $K_{\text{max}}$ ) has been known to increase with bulk density and grain size.<sup>27,28)</sup> But, the difference in bulk density was not as large as could explain

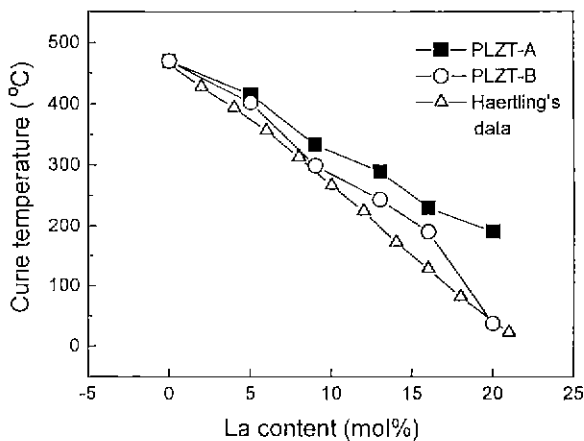


Fig. 11. Curie temperatures of PLZT-A and PLZT-B as a function of La content.

that in  $K_{max}$  and the grain size of PLZT-B was contradictorily smaller than PLZT-A below 20 mol% La. It is, therefore, necessary to find another origin to explain the difference. Comparing the peak shapes of dielectric constant, the phase transitions of PLZT-A appear to be more diffuse and hence the lower  $K_{max}$  of PLZT-A may be partially resulted from its diffuseness. Although another possible cause is supposed to be the difference in the defect structure resulted from different vacancy formulas, much study for the defect structure should be performed to clarify this phenomenon. However, it is evident that the values of  $K_{max}$  largely depend on vacancy formula.

Curie temperature ( $T_c$ ) decreases as La content increases for both series and  $T_c$  of PLZT-B still more rapidly decreases than that of PLZT-A (figure 11). The Curie temperature in perovskite ferroelectrics is well known to be directly proportional to the tetragonality of lattice.<sup>10,28,30</sup> The decreases of  $T_c$  in both series are clearly explained by the decreases of tetragonality. Similarly, the difference of decreasing slope for  $T_c$  between PLZT-A and PLZT-B can be explained by the different magnitudes of tetragonality between two series. The  $T_c$  data of PLZT, reported by Haertling and Land<sup>30</sup> who prepared PLZT ceramics by hot-pressing according to PLZT-B formula, are together plotted in figure 11 for comparison. The Curie temperatures of PLZT-B are closer to their data than PLZT-A. This means that the PLZT-B compositions prepared in this work are closer to theirs than PLZT-A and similar with compositions of conventionally prepared PLZT samples. It can be concluded that dielectric properties of PLZT are significantly affected by vacancy formulas adopted in preparation.

#### IV. Summary

The PLZT samples,  $Pb_{1-3x/2}La_xV_{x/2}(Zr_{0.2}Ti_{0.8})O_3$  and  $Pb_{1-x}La_x(Zr_{0.2}Ti_{0.8})_{1-x/4}V_{x/4}O_3$  ( $x=0.00-0.30$ ) containing A- and B-site vacancies, respectively, were prepared and investigated. The physical, structural, and dielectric properties were found to

be dependent on the vacancy formula. In both series, the main trend of structural properties agreed with the reported phase diagrams. It was found by precise comparison that the unit cell volume of PLZT-B was larger than PLZT-A, while the latter showed higher tetragonality than the former. Raman scattering revealed that two vacancy formulas had different local structures in lattice, which was distinguished by a peak at  $650\text{ cm}^{-1}$ . For dielectric properties, the remarkable differences were observed in  $T_c$  and  $K_{max}$ . In comparison with PLZT-A, the  $T_c$  of PLZT-B more rapidly decreased with increasing La content and PLZT-B showed greater  $K_{max}$  values. From these results, it can be concluded in PLZT system that some properties, specially, dielectric properties, are significantly affected by the adopted batch formulation corresponding to A- and B-site vacancy formula.

#### Acknowledgements

The present work was supported by the Basic Science Research Institute Program, Ministry of Education, 1995. Project No. BSRI-95-3404.

#### References

1. G. H. Haertling, "Electrooptic Ceramics and Devices," pp. 371-492 in *Electronic Ceramics*, Ed. by L. M. Levinson, Marcel Dekker, New York, 1988.
2. G. H. Haertling, "Improved Hot-Pressed Electrooptic Ceramics in the  $(Pb,La)(Zr,Ti)O_3$  System," *J. Am. Ceram. Soc.*, **54**[6], 303-309 (1971).
3. "Ferroelectric Ceramics," pp. 128-187, in *Ceramic Dielectrics and Capacitors*, Ed. by J. M. Herbert, Gordon and Breach Science, New York, 1985.
4. W. A. Schulze, T. G. Miller, and J. V. Biggers, "Solubility Limit of La in the Lead Zirconate-Titanate System," *J. Am. Ceram. Soc.*, **58**[1], 21-23 (1975).
5. G. R. Snow, "Fabrication of Transparent Electrooptic PLZT Ceramics by Atmosphere Sintering," *J. Am. Ceram. Soc.*, **56**[2], 91-96 (1973).
6. N. Tohge, E. Fujii, and T. Minami, "Ferroelectric Properties of PLZT Films Prepared by the Sol-Gel Process Using Chemically Modified Metal-Alkoxides," *J. Mater. Sci.: Mater. in Electronics*, **5**, 356-359 (1994).
7. Y.-J. Lee, F.-S. Yen, J.-P. Wu, and H.-I. Hsiang, "Crystallization of Lanthanum-Modified Lead Zirconate Titanate (PLZT) Using Coprecipitated Gels," *Jpn. J. Appl. Phys.*, **34**[8A], 4137-4142 (1995).
8. R. L. Holman, "The Defect Structure of 8/65/35 PLZT as Determined by Kundsen Effusion," *Ferroelectrics*, **10**, 185-190 (1976).
9. K. H. Härdtl, and D. Hennings, "Distribution of A-Site and B-Site Vacancies in  $(Pb,La)(Ti,Zr)O_3$  Ceramics," *J. Am. Ceram. Soc.*, **55**[5], 230-231 (1972).
10. G. H. Haertling, and C. E. Land, "Hot-Pressed  $(Pb,La)(Ti,Zr)O_3$  Ferroelectric Ceramics for Electrooptic Applications," *J. Am. Ceram. Soc.*, **54**[1], 1-11 (1971).
11. B.-M. Song, D.-Y. Kim, S.-I. Shirasaki, and H. Yamamura, "Effect of Excess PbO on the Densification of PLZT

- Ceramics," *J. Am. Ceram. Soc.*, **72**[5], 833-836 (1989).
12. D. R. De Villies, and P. W. Richter, "The Effect of PbO Content on a Modified Lead Titanate Ceramic," *J. Mater. Sci.*, **25**, 4140-4142 (1990).
  13. T. Tani, and D. A. Payne, "Lead Oxide Coatings on Sol-Gel-Derived Lead Lanthanum Zirconium Titanate Thin Layers for Enhanced Crystallization into the Perovskite Structure," *J. Am. Ceram. Soc.*, **77**[5], 1242-1248 (1994).
  14. A. H. Carim, "Ceramic Microstructures," pp. 119-136, in *Characterization of Ceramics*, Ed. by R. E. Loehman and L. E. Fitzpatrick, Butterworth-Heinemann, Boston, 1993.
  15. R. D. Shannon, "Revised Effective Ionic Radii and Systematic Studies of Interatomic Distances in Halides and Chalcogenides," *Acta Cryst.*, **A32**, 751-767 (1976).
  16. S.-I. Shirasaki, K. Takahashi, and K. Kakegawa, "Ferroelectric-Paraelectric Phase Transition in Lead Titanate Containing Lattice Defects," *J. Am. Ceram. Soc.*, **56**[8], 430-435 (1973).
  17. G. H. Maher, "Effect of Silver Doping on the Physical and Electrical Properties of PLZT Ceramics," *J. Am. Ceram. Soc.*, **66**[6], 408-414 (1983).
  18. R. B. Atkin, and R. M. Fulrath, "Point Defects and Sintering of Lead Zirconate-Titanate," *J. Am. Ceram. Soc.*, **54**[5], 265-270 (1971).
  19. G. H. Haertling, "Hot-Pressed Lead Zirconate-Lead Titanate Ceramics Containing Bismuth," *Am. Ceram. Soc. Bull.*, **43**[12], 875-879 (1964).
  20. B.-K. Kim, H.-O. Hamaguchi, I.-T. Kim, and K. S. Hong, "Probing of 1:2 Ordering in  $\text{Ba}(\text{Ni}_{1/3}\text{Nb}_{2/3})\text{O}_3$  and  $\text{Ba}(\text{Zn}_{1/3}\text{Nb}_{2/3})\text{O}_3$  Ceramics by XRD and Raman Spectroscopy," *J. Am. Ceram. Soc.*, **78**[11], 3117-3120 (1995).
  21. E. Husson, L. Abello, and A. Morell, "Short-Range Order in  $\text{PbMg}_{1/3}\text{Nb}_{2/3}\text{O}_3$  Ceramics by Raman Spectroscopy," *Mat. Res. Bull.*, **25**[4], 539-545 (1990).
  22. G. Burns, and B. A. Scott, "Lattice Modes in Ferroelectric Perovskites:  $\text{PbTiO}_3$ ," *Phys. Rev. B*, **7**[7], 3088-3101 (1973).
  23. G. Burns, and B. A. Scott, "Raman Spectra of Polycrystalline Solids: Application to the  $\text{PbTi}_{1-x}\text{Zr}_x\text{O}_3$  System," *Phys Rev Lett*, **25**[17], 1191-1194 (1970).
  24. A. Lurio, and G. Burns, "Vibrational Modes in  $(\text{Pb},\text{La})(\text{Zr},\text{Ti})\text{O}_3$  Ceramics," *J. Appl. Phys.*, **45**[5], 1986-1992 (1974).
  25. I. Taguchi, A. Pignolet, L. Wang, M. Proctor, F. Levy, and P. E. Schmid, "Raman Scattering from  $\text{PbTiO}_3$  Thin Films Prepared on Silicon Substrates by Radio Frequency Sputtering and Thermal Treatment," *J. Appl. Phys.*, **73**[1], 394-399 (1993).
  26. W. J. Brya, "Polarized Raman Scattering in Transparent Polycrystalline Solids," *Phys. Rev Lett.*, **26**[18], 1114-1118 (1971).
  27. K. Okazaki, and K. Nagata, "Effects of Grain Size and Porosity on Electrical and Optical Properties of PLZT Ceramics," *J. Am. Ceram. Soc.*, **56**[2], 82-86 (1973).
  28. H. T. Martirena, and J. C. Burfoot, "Grain-Size Effects on Properties of Some Ferroelectric Ceramics," *J. Phys. C: Solid State Phys.*, **7**, 3182-3192 (1974).
  29. T. Yamamoto, H. Igarashi, and K. Okazaki, "Dielectric, Electromechanical, Optical, and Mechanical Properties of Lanthanum-Modified Lead Titanate Ceramics," *J. Am. Ceram. Soc.*, **66**[5], 363-366 (1983).
  30. J. Ravez, "Relations between Curie Temperature and Chemical Bond in Octahedral Monodimensional Ferroelectrics," *Phase Transitions*, **33**, 53-64 (1991).